STABLE RECONSTRUCTION OF REGULAR 1-HARMONIC MAPS WITH A GIVEN TRACE AT THE BOUNDARY

ALEXANDRU TAMASAN*, ALEXANDRE TIMONOV†, AND JOHANN VERAS‡

Abstract. We consider the numerical solvability of the Dirichlet problem for the 1-Laplacian in a plane conformal with Euclidean. Provided that a regular solution exists, we present a globally convergent method to find it. The global convergence allows to show a local stability in the Dirichlet problem for the 1-Laplacian nearby regular solutions. Such problems occur in conductivity imaging, when knowledge of the magnitude of the current density field (generated by an imposed boundary voltage) is available inside. Numerical experiments illustrate the feasibility of the convergent algorithm in the context of the conductivity imaging problem.

Key words. 1-Laplacian, current density impedance imaging, characteristics, global convergence

AMS subject classifications. 35R30, 35J60, 31A25

1. Introduction. Let $\Omega \subset \mathbb{R}^2$ be a simply connected, bounded planar domain with piecewise C^1 boundary $\partial\Omega$, $a \in C^{1,1}(\overline{\Omega})$ with $\min_{\overline{\Omega}} a > 0$, and $f \in C^1(\partial\Omega)$. In this paper we are concerned with the numerical analysis of solutions to the Dirichlet problem for the degenerate elliptic equation of the 1-Laplacian:

$$\nabla \cdot \left(a \frac{\nabla v}{|\nabla v|} \right) = 0, \quad v|_{\partial\Omega} = f. \tag{1.1}$$

Solutions of the 1-Laplacian in (1.1) are called 1-harmonic. The name borrows from its geometric property that level sets of regular solutions of (1.1) are geodesics in the ambient plane endowed with the metric $g = a^2 I$, (where I denotes the identity metric), thus generalizing the Euclidean case $a \equiv 1$.

We call *regular solution* a function $u \in Lip(\Omega)$ with

$$\operatorname{essinf}_{\Omega} |\nabla u| > 0.$$

From [13] is known that, if it exists, a regular solution to (1.1) is unique in the class of functions in $W^{1,1}(\Omega)$ with a negligible set of singular points (where the gradient vanishes). However, there are examples of Dirichlet problems for the 1-Laplacian which may not have regular solutions. In such a case, solutions are defined in the viscosity sense [5], and (1.1) may have infinitely many such solutions none of which is regular; see the example in [17] where Ω is the unit disk, $a \equiv 1$, and $f = x^2 - y^2$ on the unit circle.

In this paper we assume that a regular solution of (1.1) exists, and provide a globally convergent numerical method to find it. As an application we are able to show conditional stability for the Dirichlet problem nearby the regular solution. To authors knowledge this is a first stability with respect to the interior data for the Dirichlet problem of the 1-Laplacian.

*Department of Mathematics, University of Central Florida, Orlando, FL, USA (tamasan@math.ucf.edu)

†Division of Mathematics and Computer Science, University of South Carolina Upstate, Spartanburg, SC, USA (atimonov@uscupstate.edu)

‡Department of Mathematics, University of Central Florida, Orlando, FL, USA (jveras@knights.ucf.edu)

§The work of the first and third authors was supported by the NSF grant DMS-1312883.

Throughout we work under the following

HYPOTHESIS 1. *The problem (1.1) has a regular solution in* $C^1(\overline{\Omega})$.

Neumann problems associated with the 1-Laplacian were first considered in [9], and Cauchy problems in [12]. The Dirichlet problem for the 1-Laplacian (1.1) was first considered in [14], where level sets of the 1-harmonic maps are shown to be geodesics in a conformal metric A locally convergent algorithm (in the sense that a first guess is sufficiently close to the sought solution) was proposed. This local convergence cannot be strengthen based on the length minimizing property alone in a general metric space: In the case of a hemisphere, infinitely many geodesics connect diametral point.

By contrast, in this paper we propose a globally convergent algorithm in the sense that it is independent on the starting guess. The method of proof relies on the fact that the level sets are characteristics of a first order PDE (see (2.2) below) to solve the two point boundary value problem for each level set by a shooting method. The merit of the paper is the global convergence, and its corollary of a local stability result. We show that the length of these characteristics depend continuously on the boundary points and directions. This is a global geometrical property that requires the convexity of the domain, and uses the fact that the Euclidean curvature of the characteristics are a priori bounded. The convergence rate of the algorithm depends on the modulus of continuity of lengths of characteristics with respect to the shooting direction.

The problem (1.1) satisfying Hypothesis 1 occurs naturally in the hybrid inverse problem of electrical conductivity imaging from minimal interior data, where $a(x)$ represents the magnitude of the current density field induced in a body by imposing the voltage f at the boundary [12, 13, 14, 15]. In such applications to a body of conductivity σ is applied a voltage f at the boundary; the voltage u then distributes inside according to the problem

$$\nabla \cdot \sigma \nabla u = 0, \quad u|_{\partial\Omega} = f. \tag{1.2}$$

In the inverse conductivity problem σ and u are unknown, but the interior data of the magnitude of the current density field $a = |\sigma \nabla u|$ can be obtained using a Magnetic Resonance technique [16]. Using $\sigma = a/|\nabla u|$ one is lead to solving (1.1). For sufficiently regular conductivities, ($\sigma \in C^{2,\alpha}(\Omega)$, $0 < \alpha < 1$, suffices) and a boundary data (in $C^{2,\alpha}(\partial\Omega)$) which is almost-two-to-one (with the exception of the connected minima and maxima it assumes the same value at exactly two boundary points) the solution of (1.2) of free of singular points [2], thus the Hypothesis 1 is automatically satisfied.

When it exists, the regular solution of (1.1) is the unique minimizer in the problem

$$\min \left\{ \int_\Omega a|\nabla u| dx : \ u \in H^1(\Omega), \ u|_{\partial\Omega} = f \right\},$$

as shown in [13], and a minimization algorithm has been proposed in [11]. In the recent work in [10], a local stability result of recovering σ from one magnitude $|J|$ without using the 1-Laplacian was shown. However, this approach ignores boundary considerations, and the absence of singular points is implicitly postulated by a restricted neighborhood of the conductivity where stability is shown. This linearized approach was originally proposed in [8] and [3] for general interior functionals, both requiring multiple interior measurements for stability.

In Section 2 we present our new algorithm which reconstructs the solution to the Dirichlet problem of the 1-Laplacian level set by level set. In Section 3 we discuss a

generic local stability result that follows from the method. In Section 4 we present two numerical experiments to illustrate the feasibility of the algorithm in its application conductivity imaging.

2. Reconstruction of level sets of u. We recall first the connection between the level sets of regular solutions of (1.1) and the characteristics of a first order PDE. By Hypothesis 1 the unknown function θ is well defined in $C^1(\overline{\Omega})$ by

$$\frac{\nabla u(x,y)}{|\nabla u(x,y)|} = \langle \cos\theta(x,y), \sin\theta(x,y)\rangle\,. \tag{2.1}$$

Since u solves problem (1.1), from (2.1) we get that θ is a solution of the first order nonlinear PDE:

$$-\theta_x \sin\theta + \theta_y \cos\theta = -\left(\ln a\right)_x \cos\theta - \left(\ln a\right)_y \sin\theta, \tag{2.2}$$

where the subscripts indicate the partial derivatives.

We solve (2.2) by the method of characteristics starting at a point on the boundary with an initial guess for the "shooting angle". By using the location where it lands on the boundary, the algorithm updates the angle. We prove convergence of the iteration to the level set of u passing through the initial point. This is the content of the two propositions below.

To fix ideas, let $\varphi : [\lambda_-, \lambda_+] \mapsto \Gamma \subset \partial\Omega$, where $\lambda_- = \min_\Omega u$ and $\lambda_+ = \max_\Omega u$, be a piecewise-smooth parametrization of a (maximal) arc of the boundary, on which $f|_\Gamma : \Gamma \to [\lambda_-, \lambda_+]$ is a bijection. Existence of the maximal arc is insured by the almost-two-to-one boundary data.

Let

$$\Theta_\lambda = \{\beta \in (-\pi, \pi] \,|\, \langle -\sin\beta, \cos\beta\rangle \cdot \vec{n}(\varphi(\lambda)) < 0\,\} \tag{2.3}$$

be the set of angles for directions $\langle -\sin\beta, \cos\beta\rangle$ pointing inside Ω. Here $\vec{n}(\varphi(\lambda))$ is the outward unit normal at $\varphi(\lambda) \in \partial\Omega$.

We consider the family (indexed in λ) of solutions to the initial value problem, each of which describe a curve originating on the boundary at $\varphi(\lambda)$ in the direction $\langle -\sin\beta, \cos\beta\rangle$:

$$\begin{cases} x_t = -\sin\theta, \\ y_t = \cos\theta, \\ \theta_t = -(\ln a)_x \cos\theta - (\ln a)_y \sin\theta, \\ (x(0), y(0)) = \varphi(\lambda), \quad \theta(0) = \beta \in \Theta_\lambda. \end{cases} \tag{2.4}$$

Since $a \in C^{1,1}(\overline{\Omega})$ is bounded away from zero, the right hand side is Lipschitz continuous and classical arguments in ODE show that there is a unique solution $t \mapsto (x(t,\lambda,\beta), y(t,\lambda,\beta))$ defined on a maximal interval $[0, \tau(\lambda,\beta))$, where

$$\tau(\lambda,\beta) := \sup\{t^* > 0 : (x(t,\lambda,\beta), y(t,\lambda,\beta) \in \Omega,\ 0 < t < t^*\}. \tag{2.5}$$

Since the curves are traced with speed one, then $\tau(s,\beta)$ also represents the length. In general $\tau(s,\beta)$ may not necessarily be finite. We will show in Proposition 2.3 below that $\tau(s,\beta)$ is finite for all $\lambda \in (\lambda_-, \lambda_+)$ and $\beta \in \Theta_\lambda$ as in (2.3). Moreover, in such a case, it follows from its definition (2.5) that $(x(\tau(\lambda,\beta),\lambda,\beta), y(\tau(\lambda,\beta),\lambda,\beta))$ is a boundary point.

The first result shows the connection between the level sets of the unknown solution u of the 1-Laplacian in (1.1), and solutions of the problem (2.4).

PROPOSITION 2.1. *Let $(\xi(t),\eta(t)) : [0,T] \mapsto \overline{\Omega}$ be a level curve of u, which solves*

$$\begin{cases} \xi'(t) = -u_y(\xi,\eta)/|\nabla u(\xi,\eta)| \\ \eta'(t) = u_x(\xi,\eta)/|\nabla u(\xi,\eta)| \\ (\xi(0),\eta(0)) = \varphi(\lambda^*),\ \lambda^* \in (\lambda_-,\lambda_+), \end{cases} \tag{2.6}$$

and define $\zeta : [0,T] \mapsto \mathbb{R}$ by

$$\zeta(t) := Arg\left\{ \frac{\nabla u}{|\nabla u|}(\xi(t),\eta(t)) \right\}. \tag{2.7}$$

Then,

(i) the curve $t \mapsto (\xi(t),\eta(t),\zeta(t))$ is a solution of (2.4) with $\beta = \zeta(0)$ and $\lambda = \lambda^*$;

(ii) a solution of (2.4) with a fixed λ and β, which intersects $(\xi(t),\eta(t),\zeta(t))$ at least once, coincides entirely with it in $\overline{\Omega}$.

Proof. Recall that $\theta = \mathrm{Arg}\frac{\nabla u}{|\nabla u|}$ in (2.1) is a solution of (2.2). From its definition in (2.7) along a level curve $t \mapsto (\xi(t),\eta(t))$, we get equality

$$\zeta(t) = \theta(\xi(t),\eta(t)). \tag{2.8}$$

Then

$$\xi'(t) = -\sin\zeta(t),\ \text{and}\ \eta'(t) = \cos\zeta(t). \tag{2.9}$$

Now use (2.2), (2.8), and (2.9) to obtain

$$\zeta'(t) = -\left(\ln a(\xi(t),\eta(t))\right)_\xi \cos\zeta(t) - \left(\ln a(\xi(t),\eta(t))\right)_\eta \sin\zeta(t), \tag{2.10}$$

thus proving (i).

To show (ii) let $t \mapsto (x(t,\lambda,\beta), y(t,\lambda,\beta), \theta(t,\lambda,\beta))$ be a solution of (2.4) for fixed λ and β, which intersects $(\xi(t),\eta(t),\zeta(t))$ at $t = t^*$. Since the right hand side of the first three equations in (2.4) is Lipschitz, then by the uniqueness part of solutions to initial value problems in ODE we have that the curve subject to

$$(x(t^*,\lambda,\beta), y(t^*,\lambda,\beta)) = (\xi(t),\eta(t)),\ \text{and}\ \theta(t^*,\lambda,\beta) = \zeta(t^*),$$

is unique. Therefore, the curves $(x(t,\lambda,\beta), y(t,\lambda,\beta), \theta(t,\lambda,\beta))$ and $(\xi(t),\eta(t),\zeta(t))$ coincide everywhere where defined in $\overline{\Omega}$. □ Note that for any fixed boundary point $\varphi(s)$, there is one specific direction $\beta(s)$ which makes the solution of (2.4) be a level curve for u, in particular of finite length. However, when solving for an arbitrary shooting direction angle β, there is no general theory to guaranty the solution is not trapped inside (case in which $\tau(s,\beta) = \infty$). We prove below the finite length property for solutions of (2.4). The proof makes essential use of the curvature bound given by the third equation in (2.4), in conjunction with the fact that Hypothesis 1.1 implies that level sets of u describe global coordinates in $\overline{\Omega}$. The following lemma is key to capturing the effect of curvature on the length.

LEMMA 2.2. *Let $f \in C^2([0,\infty))$ with $f'(t_0) \geq 0$, $|f''| < K$, and $0 < f(t) < L$. Then,*

$$L > \frac{(f'(t_0))^2}{2K}. \tag{2.11}$$

Proof. Since $f \in C^2([0,\infty))$, then there exists $t^* \in (t_0, t)$ such that

$$f(t) = f(t_0) + f'(t_0)(t-t_0) + \frac{1}{2}(t-t_0)^2 f''(t^*). \tag{2.12}$$

Using the bound on the second derivative of f we have that

$$|f(t) - f(t_0) - f'(t_0)(t-t_0)| < \frac{1}{2}(t-t_0)^2 K,$$
$$f(t) - f(t_0) > f'(t_0)(t-t_0) - \frac{1}{2}(t-t_0)^2 K.$$

Now at $t^{**} = \frac{f'(t_0)}{K} + t_0$ and using the inequality, $0 < f(t) < L$, we get that

$$L > f(t^{**}) - f(t_0) > \frac{(f'(t_0))^2}{2K}. \tag{2.13}$$

□ For the following theorems, for a fixed $\lambda \in (\lambda_-, \lambda_+)$ let

$$\beta_\lambda = \arg\left\{ \frac{\nabla u}{|\nabla u|}(\varphi(\lambda)) \right\},$$

recall the initial value problem (2.4) and the definition of $\tau(\lambda, \beta)$ in (2.5).

THEOREM 2.3. *Let $\Omega \subset \mathbb{R}^2$ be strictly convex, $a \in C^{1,1}(\overline{\Omega})$, with $\inf_\Omega |\nabla a| > 0$. Then $\tau(\lambda, \beta) < \infty$, for all $\lambda \in (\lambda_-, \lambda_+)$ and $\beta \in \Theta_\lambda$, as in (2.3).*

Proof. For the case when $\beta = \beta_\lambda$, $\tau(\beta_\lambda, \lambda) < \infty$ since all level curves of u have finite length (due to compactness).

Now take an arbitrary $\beta \in \Theta_\lambda$ with $\beta \neq \beta_\lambda$. We consider u along the corresponding solution $t \mapsto (x(t,\lambda,\beta), y(t,\lambda,\beta), \theta(t,\lambda,\beta))$ of (2.4). By Proposition 1 part (ii) we know that

$$\frac{d}{dt} u(x(t,\lambda,\beta), y(t,\lambda,\beta)) \neq 0.$$

Without loss of generality let us consider the case

$$\frac{d}{dt} u(x(t,\lambda,\beta), y(t,\lambda,\beta)) > 0, \quad 0 \leq t < \tau(\lambda,\beta). \tag{2.14}$$

We reason by contradiction: assume $\tau(\lambda,\beta) = \infty$.

Since the level sets of u describe general coordinates in $\overline{\Omega}$, with a bounded Jacobian away from zero and infinity, we may assume that level curves of u are straight lines parallel to the x-axis. (For example, the change of coordinates $[0, t(\lambda)] \times [\lambda_-, \lambda_+] \mapsto (x, y) \in \Omega$ defined by solutions of the problem

$$\begin{cases} x_t(t,\lambda) = -u_y(x,y)/|\nabla u(x,y)| \\ y_t(t,\lambda) = u_x(x,y)/|\nabla u(x,y)| \\ (x(0,\lambda), y(0,\lambda)) = \varphi(\lambda) \end{cases} \tag{2.15}$$

gives a desired diffeomorphism.) In this new coordinates we have $y_t(t) > 0$ for $t \geq 0$, and for every $\epsilon > 0$ there is an M_ϵ such that for all $t > M_\epsilon$

$$|L - y(t)| < \epsilon. \tag{2.16}$$

Let $K > \max_{\overline{\Omega}} |\nabla \ln a|$, then

$$|y_{tt}(t)| = |\sin\theta(t)||\theta_t(t)| < K. \tag{2.17}$$

Consequently, by Lemma 2.2 we have that

$$y_t^2(t) < 2K\epsilon, \quad \forall t > M_\epsilon. \tag{2.18}$$

By choosing $\epsilon < \frac{1}{4K}$ and the arc length parametrization of this curve ($x_t^2 + y_t^2 = 1$) gives the inequality

$$x_t^2(t) > \frac{1}{2} \tag{2.19}$$

for every $t > M_{\frac{1}{4K}}$. From the Mean Value Theorem one can show that $x(t)$ increases unboundedly thus contradicting the boundedness of Ω. Therefore $\tau(\lambda, \beta)$ is finite. □

THEOREM 2.4. *Assume that Ω is convex. Then the map $\beta \mapsto \tau(\lambda, \beta)$ is continuous at β_λ.*

Proof. For simplicity, we assume first that $\overline{\Omega}$ is a rectangle, say $[0, x_0] \times [0, y_0]$, in the coordinates described by the level sets of u. Or, equivalently, that the level curves of u are parallel to the x-axis. Extend the function a to the open set Ω' such that $\overline{\Omega} \subset \Omega'$, $a \in C^{1,1}(\Omega')$, and the solutions of (2.4) are defined in Ω'. Let $\epsilon > 0$ be given and let $h > 0$ be small enough and, without loss of generality, assume that $\delta := \tau(\lambda, \beta_\lambda + h) - \tau(\lambda, \beta_\lambda) > 0$ (the case when $\delta < 0$ follows similarly). By the stability with respect to t of solutions of initial value problems we have that

$$\|(x(t, \lambda, \beta_\lambda + h), y(t, \lambda, \beta_\lambda + h)) - (x(t, \lambda, \beta_\lambda), y(t, \lambda, \beta_\lambda))\|_{C^1([0, \tau(\lambda, \beta_\lambda)])} < \epsilon. \tag{2.20}$$

We will show that as $\epsilon \to 0$, then

$$\tau(\lambda, \beta_\lambda + h) - \tau(\lambda, \beta_\lambda) \to 0.$$

Observe that

$$\begin{aligned} |(x(0, \lambda, \beta_\lambda + h), y(0, \lambda, \beta_\lambda + h), \theta(0, \lambda, \beta_\lambda + h)) - \\ (x(0, \lambda, \beta_\lambda), y(0, \lambda, \beta_\lambda), \theta(0, \lambda, \beta_\lambda))| < h. \end{aligned}$$

Since $t \mapsto x(t, \lambda, \beta_\lambda + h)$ is twice continuously differentiable, then

$$\begin{aligned} &x(\tau(\lambda, \beta_\lambda + h), \lambda, \beta_\lambda + h) > \\ &x(\tau(\lambda, \beta_\lambda), \lambda, \beta_\lambda + h) + \delta x_t(\tau(\lambda, \beta_\lambda), \lambda, \beta_\lambda + h) - \frac{\delta^2}{2} K, \end{aligned}$$

where $K > \max |x_{tt}(t, \lambda, \beta)|$. Using the latter inequality and the inequality in (2.20) we get

$$\begin{aligned} &x(\tau(\lambda, \beta_\lambda + h), \lambda, \beta_\lambda + h) > \\ &x(\tau(\lambda, \beta_\lambda), \lambda, \beta_\lambda) - \epsilon + \delta[x_t(\tau(\lambda, \beta_\lambda), \lambda, \beta_\lambda) - \epsilon] - \frac{\delta^2}{2} K \\ &= x_0 - \epsilon + \delta[x_t(\tau(\lambda, \beta_\lambda), \lambda, \beta_\lambda) - \epsilon] - \frac{\delta^2}{2} K. \end{aligned}$$

Since, $x_0 = x(\tau(\lambda, \beta_\lambda + h), \lambda, \beta_\lambda + h)$ and $x_t(\tau(\lambda, \beta_\lambda), \lambda, \beta_\lambda) > 0$, then

$$0 > -\epsilon + \delta[x_t(\tau(\lambda, \beta_\lambda), \lambda, \beta_\lambda) - \epsilon] - \frac{\delta^2}{2}K \tag{2.21}$$

and

$$\begin{aligned}\delta &< \frac{1}{K}\left[x_t(\tau(\lambda, \beta_\lambda), \lambda, \beta_\lambda) - \epsilon - \sqrt{[x_t(\tau(\lambda, \beta_\lambda), \lambda, \beta_\lambda) - \epsilon]^2 - 2\epsilon K}\right] \\ &= \frac{2\epsilon}{x_t(\tau(\lambda, \beta_\lambda), \lambda, \beta_\lambda) - \epsilon + \sqrt{[x_t(\tau(\lambda, \beta_\lambda), \lambda, \beta_\lambda) - \epsilon]^2 - 2\epsilon K}} \\ &< \frac{2\epsilon}{x_t(\tau(\lambda, \beta_\lambda), \lambda, \beta_\lambda) - \epsilon}.\end{aligned}$$

Thus continuity follows, since, if $\epsilon \to 0$ then, $\tau(\lambda, \beta_\lambda + h) - \tau(\lambda, \beta_\lambda) \to 0$.
□

The continuity of $\tau(\lambda, \beta)$ at β_λ yields the following.

COROLLARY 2.5. *Under the hypotheses of Theorem above, for each $\lambda \in (\lambda_-, \lambda_+)$ consider the map $F_\lambda : \Theta_\lambda \mapsto \mathbb{R}$ defined by*

$$F_\lambda(\beta) := u\left(x(\tau(\lambda, \beta), \lambda, \beta), y(\tau(\lambda, \beta), \lambda, \beta)\right) - \lambda, \tag{2.22}$$

where $(x(\tau(\lambda, \beta), \lambda, \beta), y(\tau(\lambda, \beta), \lambda, \beta)$ is the corresponding solution of (2.4), and Θ_λ as in (2.3). Then $\beta \mapsto F_\lambda(\beta)$ is a continuous at β_λ.

The algorithm and its convergence rely on the following properties of F.

PROPOSITION 2.6. *(i)$F_\lambda(\beta) = 0$ if and only if $\beta = \beta_\lambda$.*

(ii) There exist α and β such that

$$F_\lambda(\alpha) < 0 < F_\lambda(\beta). \tag{2.23}$$

Proof. First we prove statement (i). Let $\beta \in \Theta_\lambda$ such that

$$F_\lambda(\beta) = 0. \tag{2.24}$$

Thus, $\lambda = u(x(\tau(s, \beta), s, \beta), y(\tau(s, \beta), s, \beta))$. By Rolle's Theorem $\exists t^* \in (0, \tau(\lambda, \beta))$ such that

$$\frac{d}{dt}u(x(t^*, \lambda, \beta), y(t^*, \lambda, \beta)) = 0. \tag{2.25}$$

Consequently,

$$\theta(t^*, \lambda, \beta) = \operatorname{Arg}\left\{\frac{\nabla u}{|\nabla u|}(x(t^*, \lambda, \beta), y(t^*, \lambda, \beta))\right\}. \tag{2.26}$$

Therefore, by Proposition 2.1 $(x(t, \lambda, \beta), y(t, \lambda, \beta))$ is a level curve and

$$\beta = \beta_\lambda. \tag{2.27}$$

The converse follows directly from Proposition 2.1.

The proof of (ii) is as follows. Let $\alpha, \beta \in \Theta_\lambda$ such that

$$\alpha < \beta_\lambda < \beta.$$

Without loss of generality assume that $F_\lambda(\alpha)$, and $F_\lambda(\beta)$ are negative. Then, either the curve $(x(t,\lambda,\alpha), y(t,\lambda,\alpha))$ or the curve $(x(t,\lambda,\beta), y(t,\lambda,\beta))$ intersects, in $\overline{\Omega}$, the level curve of u corresponding to λ. Then, assume $(x(t,\lambda,\beta), y(t,\lambda,\beta))$ intersects the level curve at $t = t_1$. By the same argument of the proof of statement (i) in this Proposition, there is a $t^* \in (0, t_1)$ such that

$$\frac{d}{dt} u(x(t^*,\lambda,\beta), y(t^*,\lambda,\beta)) = 0. \tag{2.28}$$

The latter implies that the curve $(x(t,\lambda,\beta), y(t,\lambda,\beta))$ is a level curve which is a contradiction, since

$$\beta > \beta_\lambda. \tag{2.29}$$

□

The following algorithm recovers the λ-level set of u, for $\lambda \in (\lambda_-, \lambda_+)$ fixed.

Algorithm: We will recursively define the following sequences. Let $\alpha_1 < \alpha_1' \in \Theta_\lambda$ be the angles given by proposition 2.6 such that

$$F_\lambda(\alpha_1) < 0 < F_\lambda(\alpha_1'). \tag{2.30}$$

Consider, for the natural number n, the bisector angle

$$\gamma_n = \frac{\alpha_n + \alpha_n'}{2}. \tag{2.31}$$

For each member of the sequences (α_n) and (α_n'),

- if $F_\lambda(\gamma_n) \le 0$, let $\alpha_{n+1} = \gamma_n$ and $\alpha_{n+1}' = \alpha_n'$, or
- if $F_\lambda(\gamma_n) > 0$, let $\alpha_{n+1}' = \gamma_n$ and $\alpha_{n+1} = \alpha_n$.

Note the ordering

$$\alpha_1 \le \alpha_n \le \alpha_{n+1} < \alpha_{n+1}' \le \alpha_n' \le \alpha_1' \tag{2.32}$$

and

$$\alpha_{n+1}' - \alpha_{n+1} = \frac{\alpha_n' - \alpha_n}{2}. \tag{2.33}$$

Consequently,

$$\alpha_{n+1}' - \alpha_{n+1} = \frac{\alpha_1' - \alpha_1}{2^n}. \tag{2.34}$$

Therefore, the sequences (α_n) and (α_n') both converge to the same angle γ. The continuity of F_λ at β_λ and the inequality in (2.30) imply that

$$F_\lambda(\alpha_n) \to F_\lambda(\gamma) = 0 \quad \text{and} \quad F_\lambda(\alpha_n') \to F_\lambda(\gamma) = 0, \tag{2.35}$$

and by Proposition 2.6

$$\gamma = \beta_\lambda. \tag{2.36}$$

Proposition 2.1 guarantees that the curve $(x(t,\lambda,\gamma), y(t,\lambda,\gamma))$ is the level curve of u corresponding to $u = \lambda$.

Note that it is the modulus of continuity of F which determines the rate of convergence of our algorithm.

3. On the stability of the method. In this section we discuss a conditional stability result.

An additional differentiation in the first two equations of (2.4) and substitution into the third equation, enables us to eliminate θ. Our method, in fact, solves the family of two point boundary value problems

$$(3.1)\quad \begin{cases} x_{tt} = y_t\left[(\ln a)_x y_t - (\ln a)_y x_t\right] \\ y_{tt} = -x_t\left[(\ln a)_x y_t - (\ln a)_y x_t\right] \\ (x(0), y(0)) = \varphi(\lambda), \quad (x(L), y(L)) = (x(\tau(\lambda,\beta),\lambda,\beta), y(\tau(\lambda,\beta),\lambda,\beta)). \end{cases}$$

In general, a two point boundary value problem may have no solutions, unique solution or infinitely many solutions. However, sufficient conditions for existence, uniqueness and continuous dependence on the data have been long known, see e.g. [7]. In what follows we do not revisit the stability issue of the two point boundary value problem but rather assume that our system (3.1) obeys some sufficient conditions (one such example can be obtained by the reduction of (3.1) to a Fredholm integral system of second type) that yield:

HYPOTHESIS 2. *For every $\epsilon > 0$ there is a $\delta > 0$ such that if*

$$(3.2)\qquad \|\tilde{a} - a\|_{C^{1,1}(\overline{\Omega})} < \delta \text{ and } \|\tilde{f} - f\|_{C^0(\Gamma)} < \delta,$$

then

$$(3.3)\qquad \max_{t\in[0,L]} (|x(t) - \tilde{x}(t)| + |y(t) - \tilde{y}(t)|) < \epsilon.$$

Let us consider the class $\mathscr{C}$ of pairs $(a, f) \in C^{1,1}(\overline{\Omega}) \times C^1(\Gamma)$, for which the problem (1.1) has a regular solution satisfying Hypotheses 1 and 2. Within the class $\mathscr{C}$, our method is conditionally stable in the following sense:

PROPOSITION 3.1 (Conditional Stability). *For every $\epsilon > 0$ there is a $\delta > 0$ such that if $(a, f), (\tilde{a}, \tilde{f}) \in \mathscr{C}$ with*

$$(3.4)\qquad \|\tilde{a} - a\|_{C^{1,1}(\overline{\Omega})} < \delta \text{ and } \|\tilde{f} - f\|_{C^0(\Gamma)} < \delta,$$

then

$$(3.5)\qquad \|u - \tilde{u}\|_{C^0(\overline{\Omega})} < \epsilon.$$

Proof. Let $P \in \overline{\Omega}$. Consider the following curves:

- the level curve $[0, L] \ni t \mapsto (x(t), y(t))$ corresponding to $u(P)$, and
- the level curve $[0, L] \ni t \mapsto (x^*(t), y^*(t))$ of $\tilde{u}$ with $(x(0), y(0)) = (x^*(0), y^*(0))$.

For $\epsilon > 0$ and P given, let $P^* \in \{(x^*(t), y^*(t)) : t \in [0, L]\}$ be the closest point to P. From Hypothesis 2 there is a $0 < \delta < \epsilon/2$ small enough with the property: if

$$(3.6)\qquad \|\tilde{a} - a\|_{C^{1,1}(\overline{\Omega})} < \delta \text{ and } \|\tilde{f} - f\|_{C^0(\Gamma)} < \delta,$$

then

$$(3.7)\qquad \sup_{t\in[0,L]} \sqrt{|x(t) - x^*(t)|^2 + |y(t) - y^*(t)|^2} < \frac{\epsilon}{2L_{\tilde{u}}},$$

where $L_{\tilde{u}}$ is the $\max_{\overline{\Omega}} |\nabla \tilde{u}|$. Consequently, $\text{dist}(P, P^*) < \frac{\epsilon}{2L_{\tilde{u}}}$. We estimate

$$\begin{aligned} |u(P) - \tilde{u}(P)| &= |f(x(0), y(0)) - \tilde{u}(P)| \\ &\leq |\tilde{f}(x(0), y(0)) - \tilde{u}(P)| + |f(x(0), y(0)) - \tilde{f}(x(0), y(0))| \\ &\leq \delta + |\tilde{u}(P^*) - \tilde{u}(P)| < \frac{\epsilon}{2} + L_{\tilde{u}} \text{dist}(P^*, P) < \epsilon. \end{aligned}$$

Since P were arbitrary in $\overline{\Omega}$, then

$$\|u - \tilde{u}\|_{C^0(\overline{\Omega})} < \epsilon. \tag{3.8}$$

□

4. Numerical Results. In this section we present two numerical reconstructions of some conductivities based on the algorithm above. Figure 1 illustrates the two conductivities which are to be reconstructed from the data. Also, figure 2 shows the difference of the calculated solution of the conductivity equation (1.2) (for each conductivity) and the harmonic function with the same boundary data.

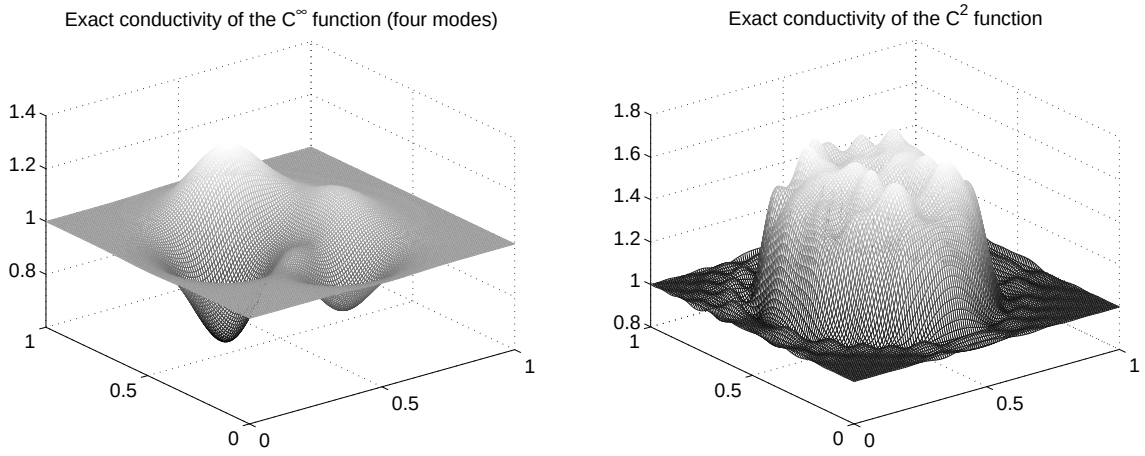

FIG. 1. *The original conductivity distribution maps: the four modes (left) and the cross section of a C^2 approximation of a human brain (right).*

4.1. Data. The magnitude of the current density, a, for the numerical experiments is obtained numerically.

We solve the Dirichlet problem (1.2) for two different conductivities by using the finite element method in MATLAB's PDE toolbox. The domain Ω is the unit box $[0,1] \times [0,1]$, and the boundary voltage $f(x,y) = y$ is applied at the boundary. The first conductivity map is smoothly defined by the C^∞ (four modes) function

$$\sigma(x,y) = 1 + 0.3 \cdot (A(x,y) - B(x,y) - C(x,y)), \tag{4.1}$$

where

$$A = 0.3 \cdot [1 - 3(2x-1)]^2 \cdot e^{-9\cdot(2x-1)^2 - (6y-2)^2},$$

$$B = \left[\frac{3(2x-1)}{5} - 27 \cdot (2x-1)^3 - [3 \cdot (2y-1)]^5\right] \cdot e^{-\left[9\cdot(2x-1)^2 + 9\cdot(2y-1)^2\right]},$$

$$C = e^{-[3\cdot(2x-1)+1]^2 - 9\cdot(2y-1)^2};$$

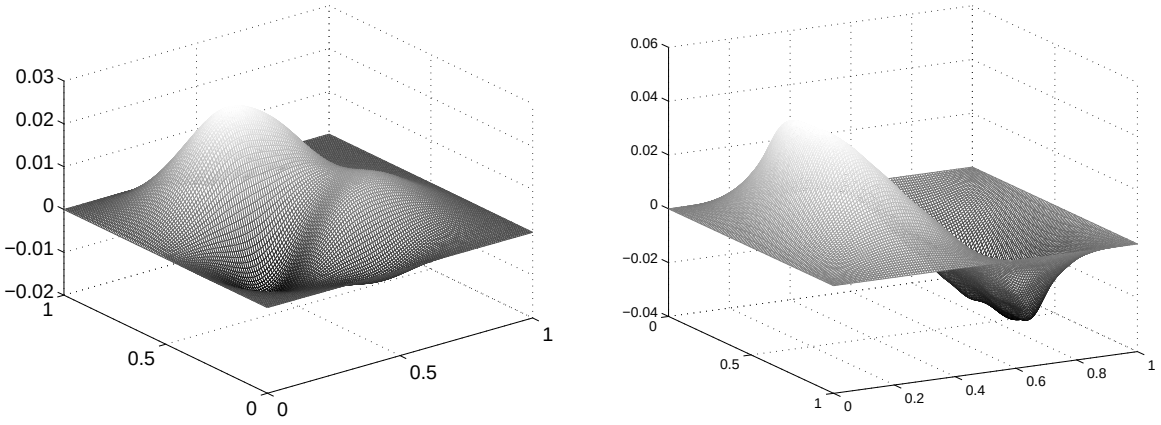

FIG. 2. *The figure illustrates $u(x,y) - y$, where $u(x,y)$ is the solution of (1.2) subject to $f(x,y) = y$ and the conductivities: the C^∞ function (left) and the C^2 function (right).*

see the left image in Figure 1. The second conductivity is a least square approximation of C^2 B-splines of a piecewise-smooth function given by a CT image of a cross-section of a human brain. This level of smoothness is needed to meet the theory requirements. The approximating function has the form

$$\sigma(x,y) = \sum_{i=1}^{22}\sum_{j=1}^{18} \alpha_{ij} B(x - x_j) B(y - y_i), \tag{4.2}$$

and it is shown in Figure 1 on the right.

The gradient of the potential ∇u is computed via finite difference. The interior data $a = \sigma|\nabla u|$ is computed in $[0,1] \times [0,1]$, see figure below.

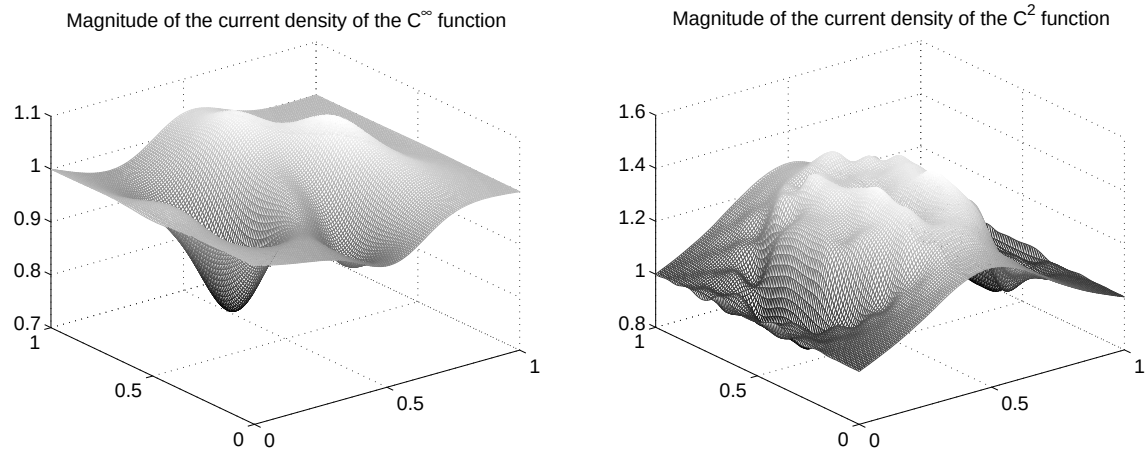

FIG. 3. *Magnitude of the current density of the C^∞ (four modes) (left) and the C^2 function (right) generated over the box $[0,1] \times [0,1]$.*

4.2. Finding β_λ. The algorithm in section 2 finds the root β_λ of the function $F_\lambda(\beta)$ in (2.22), which together with $(x(0,\lambda,\beta_\lambda), y(0,\lambda,\beta_\lambda))$ give the initial condition of a level curve of u which solves (2.4). To find β_λ numerically, we use the boundary points which are joined by the level curve of u corresponding to λ, say (x_1, y_1) and (x_2, y_2). Note that the boundary data is almost-two-to-one and these points are the unique points such that $f(x_1, y_1) = f(x_2, y_2)$.

The method shown here is similar to a bi-section searching algorithm. The novelty is the criterion which ensures convergence. The iterative process is as follows. Assume that $x_1 = 0$ and $y_1 \in (0, 1)$. To initialize the process we solve (2.4) twice: once subject to (x_1, y_1, α_0) and next subject to (x_1, y_1, α_0'), where $\alpha_0, \alpha_0' \in (-\pi, 0)$ are initial guesses such that

$$F_\lambda(\alpha_0) < 0 < F_\lambda(\alpha_0'). \tag{4.3}$$

The next angle is $\gamma_0 = \frac{\alpha_0+\alpha_0'}{2}$. Solve (2.4) subject to (x_1, y_1, γ_0). If $F_\lambda(\gamma_0) < 0$, then let the next angles $\alpha_1 = \gamma_0$ and $\alpha_1' = \alpha_0'$. Otherwise, let $\alpha_1 = \alpha_0$ and $\alpha_1' = \gamma_0$. Assign the new angle, $\gamma_1 = \frac{\alpha_1+\alpha_1'}{2}$. Solve (2.4) subject to (x_1, y_1, γ_1). Repeat this scheme n number of times, so that

$$|\beta_\lambda - \gamma_n| < |\alpha_0 - \alpha_0'| \frac{1}{2^n}. \tag{4.4}$$

The plots in figure 4 show a numerical example of the convergence rate of this method for the voltage potential generated with the $\sigma \in C^2$ example.

We can also use the continuity (for $\delta > 0$ small enough, β_λ is close to $\beta_{\lambda+\delta}$) to expedite the convergence rate of the method when from level to level set by using the already calculated values.

In Figure 4 the reconstructed level curve passing through $(x_1, y_1) = (0, 0.6)$, which corresponds to the voltage potential generated in brain experiment $\sigma \in C^2$. The initial angles are $\alpha_0 = -\frac{2\pi}{3}$ and $\beta_0 = -\frac{\pi}{10}$. The box on the right shows a plot of the error versus the number of iterations. The error shown is a discrete version of

$$\|(x(t,\lambda,\gamma_i), y(t,\lambda,\gamma_i), \theta(t,\lambda,\gamma_i)) - (x(t,\lambda,\gamma_{i-1}), y(t,\lambda,\gamma_{i-1}), \theta(t,\lambda,\gamma_{i-1}))\|_\infty.$$

The calculated error at the 11-th iteration is $2.5 \cdot 10^{-4}$.

4.3. Numerical experiments. The numerical examples below consider two instances of the 1-Laplacian coming from the inverse conductivity problem with the data described in 4.1.

Given the function a in a unit box $[0, 1] \times [0, 1]$, we solve (2.4) using the adaptive Runge-Kutta-Fehlberg ODE solver for m characteristics subject to the initial conditions of the corresponding level curves of u, the voltage potential, found using the bi-section method in section 4.2,

$$x_j(0) = 0, y_j(0) = s_j, \theta_j(0) = \beta_{s_j}, \tag{4.5}$$

where $s_j = \frac{j}{m-1}$, and $j = 0, 2, \ldots, m-1$. Since $f(x, y) = y$, then $\beta_{s_0} = \beta_{s_{m-1}} = -\frac{\pi}{2}$.

The third equation in (2.4) contains the derivative of a in the direction of the unit vector $\eta = \langle \cos\theta, \sin\theta \rangle$:

$$\frac{d\theta}{dt} = -\partial_\eta \ln a. \tag{4.6}$$

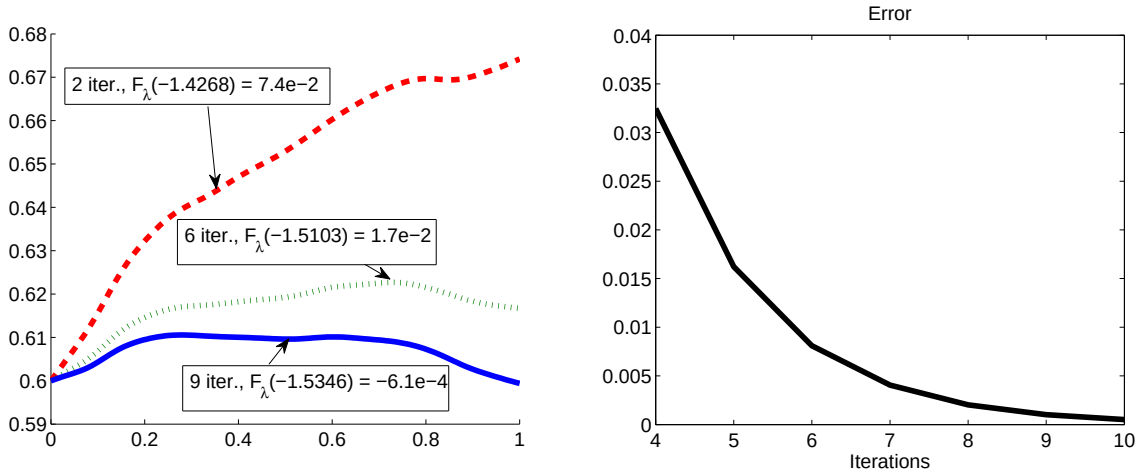

FIG. 4. *The plots in the left box show a few iterations in finding the level curve passing through* $(x_1, y_1) = (0, 0.6)$.

In order to decrease the error made in differentiating $\ln a$ we use the center difference for the directional derivative:

$$\partial_\eta \ln a(x_j(t_{j_k}), y_j(t_{j_k})) = \frac{1}{2h}\left[\ln a(x^{j_k}_{j+h}, y^{j_k}_{j+h}) - \ln a(x^{j_k}_{j-h}, y^{j_k}_{j-h})\right], \tag{4.7}$$

where

$$\begin{aligned} x^{j_k}_{j+h} &= x_j(t_{j_k}) + h \cdot \cos\theta_j(t_{j_k}), \\ x^{j_k}_{j-h} &= x_j(t_{j_k}) - h \cdot \cos\theta_j(t_{j_k}), \\ y^{j_k}_{j+h} &= y_j(t_{j_k}) + h \cdot \sin\theta_j(t_{j_k}), \\ y^{j_k}_{j-h} &= y_j(t_{j_k}) - h \cdot \sin\theta_j(t_{j_k}). \end{aligned}$$

In all the numerical experiments the value of $\ln a$ (or a) at a point is interpolated by the bi-quintic piecewise Lagrange polynomials for points away from the boundary, and the bi-cubic or bi-linear interpolation for points near the boundary.

The characteristics are equipotential lines. The value of the potential along each characteristic is determined by the voltage potential at the boundary. Let

$$\Lambda_j(t) = (x_j(t), y_j(t)),\ j \in \{0, 1, \ldots, m-1\}, t \in [0, \tau_j], \tag{4.8}$$

denote the equipotential line, which solves (2.4) subject to (4.5), and

$$\zeta_i(\xi) = (\hat{x}_i(\xi), \hat{y}_i(\xi)), \xi \in [0, \alpha_i],\ i \in \{0, 1, \ldots, n-1\}, \tag{4.9}$$

denote a smooth non-characteristic curve, which is transversal to each $\Lambda_j, j = 0, 1, \ldots, m-1$. At the point of intersection we have

$$\begin{cases} 0 = u_x \frac{dx_j}{dt} + u_y \frac{dy_j}{dt}, \\ u_\xi = u_x \frac{d\hat{x}_i}{d\xi} + u_y \frac{d\hat{y}_i}{d\xi}, \end{cases} \tag{4.10}$$

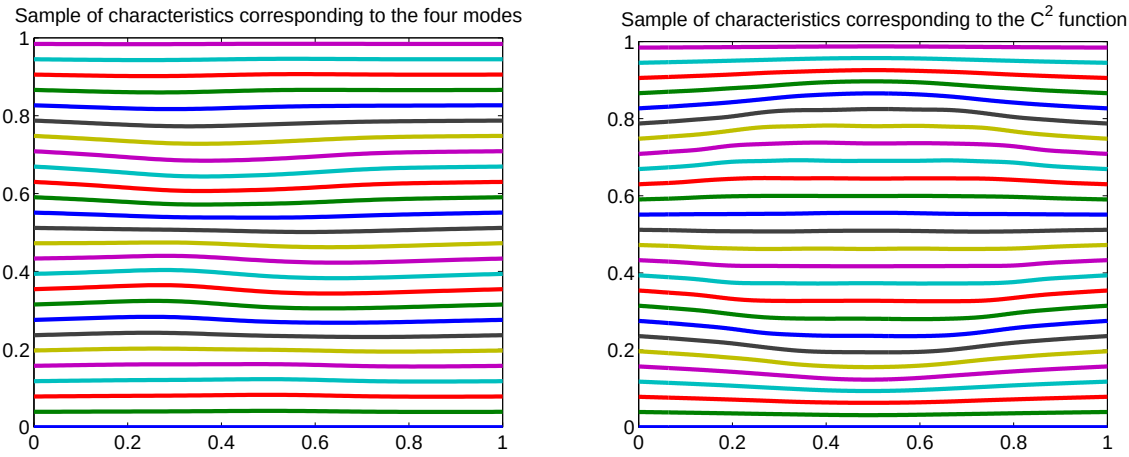

FIG. 5. *The top images show a sample of the characteristics (level curves) of the voltage potential generated by the four modes (left) and the C^2 function (right) reconstructed from the interior data, a, measured in* $[0,1]\times[0,1]$.

and

$$\nabla u = \frac{u_\xi}{\frac{dy_j}{dt}\frac{d\hat{x}_i}{d\xi} - \frac{dx_j}{dt}\frac{d\hat{y}_i}{d\xi}} \left\langle \frac{dy_j}{dt}, -\frac{dx_j}{dt} \right\rangle. \tag{4.11}$$

The non-characteristic curves of (4.9) are obtained by one dimensional interpolation in between points lying on different characteristics. The derivative u_ξ at the node where Λ_j intersects ζ_i, is computed via the Lagrange polynomial interpolation along ζ_i.

In the particular case in which the characteristic curves are graphs, say $\left|\frac{dx_j}{dt}\right| > 0$, $j = 0, 1, \ldots, m-1$, the conductivity is computed on a grid. The first component of each characteristic is regarded as the independent variable x and the second component can be expressed as a function $y_j = \phi_j(x)$, $j = 0, 1, \ldots, m-1$. Thus, by letting $x^k = \frac{k}{n-1}, k = 0, 1, \ldots, n-1$ we approximate the values of $y_j^k = \phi_j(x^k), j = 0, 1, \ldots, m-1, k = 0, 1, \ldots, n-1$ via fifth degree piecewise Lagrange polynomials. Note that for a fixed j, u is constant along the points (x^k, y_j^k), $k = 0, 1, \ldots, n-1$. Then there is a function ψ such that $u_k = \psi(y; x_k)$, for $k = 0, 1, \ldots, n-1$, whose values are known at (x^k, y_j^k). Now, by letting $y^l = \frac{l}{p-1}, l = 0, 1, \ldots, p-1$ we approximate the values $u_k^l = \psi(y^l; x^k)$ via fifth degree piecewise Lagrange polynomials. Therefore, u is approximated on the p by n rectangular grid (x^k, y^l), where $k = 0, 1, \ldots, n-1$, and $l = 0, 1, \ldots, p-1$.

We reconstruct the voltage potential for each conductivity with Gaussian noise added to the data, the magnitude of the current density. In figure 6 we show the reconstruction of the difference of the voltage potential and the harmonic solution for the noiseless data. The L_1 relative errors for the reconstructed voltage potentials from noiseless data corresponding to the C^∞ function is 1.2691×10^{-5}, and the C^2 function is 1.4798×10^{-4}. In figure 7 we plot the error of the voltage potential reconstructions from data with various degrees of Gaussian noise.

One recovers the conductivity on the characteristics of u. The gradient of the voltage potential is computed using (4.11). In the specific case in which the equipo-

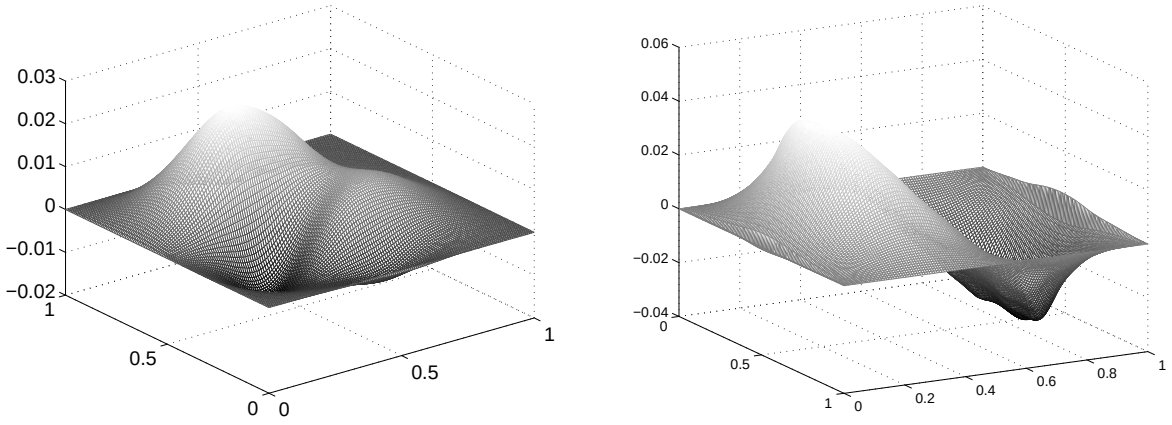

FIG. 6. *The images show the reconstruction of the difference $u(x,y) - y$ for each conductivity from noiseless data: C^∞ function (left) and C^2 function (right).*

tential curves are graphs, the conductivity is computed on the rectangular grid from step 2, $(x^k, y^l), k = 0, 1, 2, \ldots, n-1, l = 0, 1, 2, \ldots, p-1$, using the formula

$$\sigma(x^k, y^l) = \frac{a(x^k, y^l)}{|\nabla u|(x^k, y^l)}. \tag{4.12}$$

The gradient of the voltage potential of the reconstruction of the conductivities shown in figure 8 were computed via fintie differences.

4.4. Remarks on numerical stability and applications to noisy data. Sharp elliptic regularity estimates of Agmon-Douglas-Nirenberg [1] show that we cannot expect stability estimates in the same order of regularity for the 1-Laplacian, due to the degeneracy in ellipticity. Our Proposition 3.1, even in the case of exact boundary data, show a loss of two derivatives in the error estimates of the solution versus the interior data. However, the numerical experiments below, see Figure 7, show better numerical stability behaviour, equivalent to the loss of one derivative.

5. Conclusion. We presented a globally convergent algorithm which solves the Dirichlet problem for the 1-Laplacian in two dimensions by recovering the regular solution (assumed to exist) level set by level set. Such a problem occurs in the inverse hybrid problem of recovering the electrical conductivity of a body when the magnitude of the current density field, obtained by maintaining a fix boundary voltage, is given inside.

The method requires the interior coefficient be of Lipschitz gradient and does not work (in theory) for rougher data. Due to the degeneracy in ellipticity a loss of derivatives in the stability estimates are expected. We show a conditional stability result which estimates the continuous norm of the error in solution with the $C^{1,1}$-norm of error in the data. However, in numerical experiments it seems that a stability estimate with one loss of derivative may be possible.

Feasibility of the method is numerically illustrated on two examples coming from a hybrid problem in conductivity imaging.

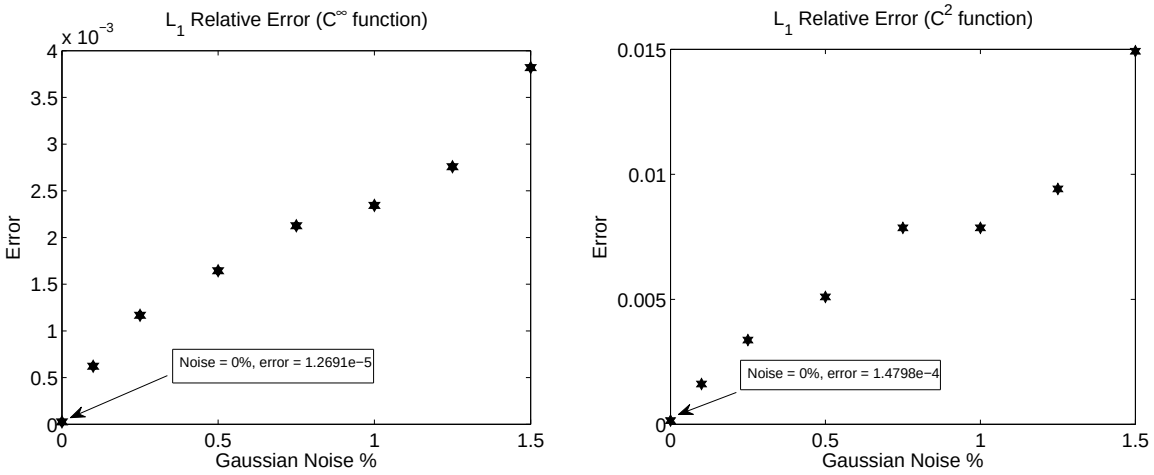

FIG. 7. *L_1 relative error of the voltage potential reconstructed from noisy data for each corresponding conductivity.*

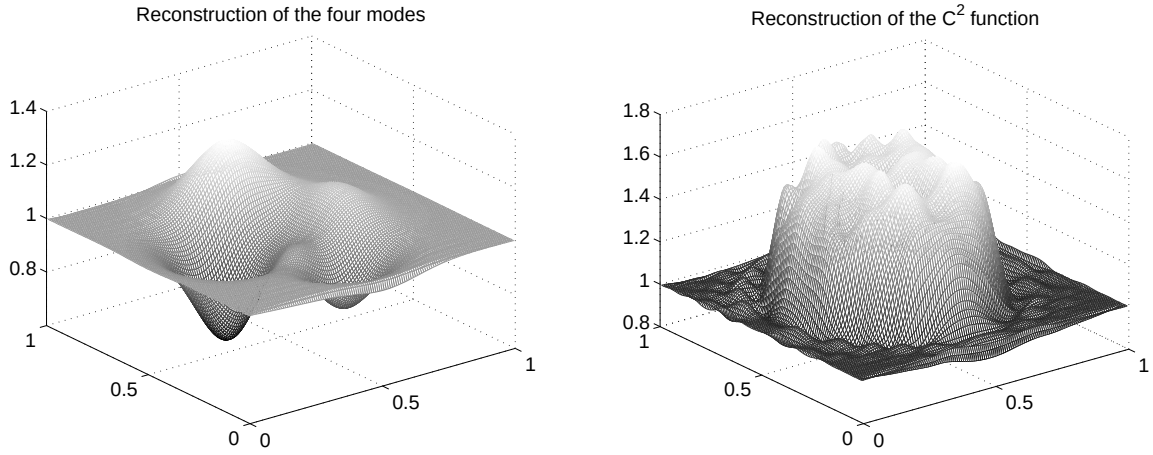

FIG. 8. *The images show the reconstruction of the four modes (left) and the C^2 function (right) reconstructed from the interior data measured in $[0,1]\times[0,1]$. The L_1 relative error for the reconstruction of the four modes and the C^2 function are 0.105% and 0.522%, respectively.*

REFERENCES

[1] S. AGMON, DOUGLIS A., AND NIRENBERG L, *Estimates near the boundary for solutions of elliptic partial differential equations satisfying general boundary conditions.* I. Comm. Pure Appl. Math. **12**(1959) 623-727. II. Comm. Pure Appl. Math. **17**(1964) 35-92.

[2] G. ALESSANDRINI AND R. MAGNANINI, *The index of isolated critical points and solutions of elliptic equations in the plane*, Ann. Suola Norm. Sup. Pisa Cl. Sci. (4), **94** (1992), pp. 567–589.

[3] F. Monard and G. Bal *Inverse diffusion problems with redundant internal information*, Inverse Probl. Imaging **6** (2012), no. 2, 289313.

[4] C. DE BOOR, *Bicubic spline interpolation*, J. Math. Phis., **41** (1962).

[5] M. G. CRANDALL, H. ISHII, AND P. -L. LIONS, *Users guide to viscosity solutions of second order partial differential equations*, Bull. Amer. Math. Soc. **27**(1992), 167

[6] D. GILBARG AND N. S. TRUDINGER, *Elliptic Partial Differential Equations*, 2nd ed., Springer-

Verlag, NY, 2001.
[7] H. B. Keller, *Numerical methods for two-point boundary value problems*, Dover Publications Inc., New York, 1992.
[8] P. Kuchment and D. Steinhauer, *Stabilizing inverse problems by internal data*, Inverse Problems **28**(2012), no. 8, 084007
[9] S. Kim, O. Kwon, J. K. Seo, and J. R. Yoon, *On a nonlinear partial differential equation arising in magnetic resonance electrical impedance tomography*, SIAM J. Math. Anal., **34** (2002), pp. 511–526.
[10] C. Montalto and P. Stefanov, *Stability of coupled-physics inverse problems with one internal measurement*, Inverse Problems **29**(2013), 125004 doi:10.1088/0266-5611/29/12/125004
[11] A. Moradifam, A. Nachman, and A. Timonov, *A convergent algorithm for the hybrid problem of reconstructing conductivity from minimal interior data*, Inverse Problems **28** (2012), no. 8, 084003, 23 pp.
[12] A. Nachman, A. Tamasan, and A. Timonov, *Conductivity imaging with a single measurement of boundary and interior data*, Inverse Problems, **23** (2007), pp. 2551–2563.
[13] A. Nachman, A. Tamasan, and A. Timonov, *Recovering the conductivity from a single measurement of interior data*, Inverse Problems, **25** (2009) 035014 (16pp).
[14] A. Nachman, A. Tamasan, and A. Timonov, *Reconstruction of planar conductivities in subdomains from incomplete data*, SIAM J. Appl. Math. **70**(2010), 3342 –3362.
[15] A. Nachman, A. Tamasan, and A. Timonov, *Current density impedance imaging* in Tomography and inverse transport theory, 135149, Contemp. Math. **559**, AMS, Providence, RI, 2011
[16] G. C. Scott, M. L. Joy, R. L. Armstrong, and R. M. Henkelman, *Measurement of nonuniform current density by magnetic resonance*, IEEE Trans. Med. Imag., **10** (1991), pp. 362–374
[17] P. Sternberg and W. P. Ziemer, *Generalized motion by curvature with a Dirichlet condition*, J. Differ. Eq., **114** (1994), pp. 580–600.
[18] A. Tamasan and J. Veras, *Conductivity imaging by the method of characteristics in the 1-Laplacian*, Inverse Problems **28** (2012), no. 8, 084006, 13 pp.